Sl. No.	IIT Ropar List of Recent Publications with Abstract Coverage: September, 2022
1.	6- Mesenchymal stem cells: Novel avenues in combating COVID-19 A Mukherjee, B Das - Stem Cells and COVID-19: Book Chapter, 2022 **Abstract:** From December 2019, COVID-19 pandemic has hit the human civilization in an unprecedented way. It has taken more than five million lives in just a span of two years. Two major mechanisms via which COVID-19 affects us are either via direct respiratory disorder and lung failure or otherwise via delayed flare of immune systems more prevalently known as the cytokine storm. Mesenchymal stem cells (MSCs) can be a potential therapeutic agent against mortality and morbidity of COVID-19 via direct differentiation into pulmonary epithelial cells as well as via antiinflammatory paracrine activities. MSCs are also can be useful to replicate COVID-19 infection in an in vitro organ model. In current study, we are systematically reviewing and finding out the potential applications of MSCs which could help mankind to combat COVID-19.
2.	A Low-Overhead PUF Based Hardware Security Technique to Prevent Scan Chain Attacks for Industry-Standard DFT Architecture S Chittoriya, KK Jha, DM Das, R Sharma - IEEE 65th International Midwest Symposium on Circuits and Systems (MWSCAS), 2022 **Abstract:** A PUF based hardware security circuit (PBHSC) is proposed for testable ICs containing design for testability (DFT) circuitry. DFT techniques such as scan chain enhance the controllability and observability of internal nodes of an IC, which leads to vulnerabilities such as IP theft or tampering. The proposed solution restricts unauthorized access to DFT structures by inhibiting enable pin of test circuitry. A PUF based lock and key mechanism enable test circuitry only upon successful authentication of the user. Area and power consumption overheads and the latency of the proposed technique are insignificant as these are independent of the size of the circuit under test (CUT). The proposed technique is compatible with the industry-standard DFT architectures such as scan-chain, BIST, JTAG, etc. The proposed design is implemented on Zynq UltraScale + ZCU102 FPGA and Vivado design suite. Proposed PBHSC utilizes 11 LUTs, 7 registers, 1 clock-buffer, 1 clock-cycle is used to produce output, and consumes 18mW power at 100MHz.
3.	A Remote Sensing based study of Tropospheric Ozone Concentration amid COVID-19 Lockdown over India using Sentinel-5P Satellite Data AR Reshi, M Moniruzzaman, A Tripathi, RK Tiwari, KR Rahaman - Geocarto International, 2022 **Abstract:** Amid the COVID-19 crisis, governments all over the world, and not excluding India, took to lockdown measures to deaccelerate the spread of the COVID-19 virus. This led to reduction of atmospheric pollution by declining the harmful Nitrogen and Sulphur Oxide (NO_X and SO_X) concentrations. However, one hand while the stratospheric Ozone (O_3) showed repair, the lower atmospheric O_3 concentrations demonstrated a remarkable increase during lockdown phase over India. This study aims to estimate the O_3 concentration during the Covid-19 lockdown over Pune city in India using freely available Sentinel-5P satellite datasets. The study makes use of the Ordinary Least Squares (OLS) and Random Forest (RF) regressions and

	compares the findings of the two algorithms based on estimation results. This study utilizes lower atmospheric O_3 concentration data from Sentinel-5P satellite of the European Space Agency (ESA) over the Indian mainland for a month of lockdown scenario (March 22nd, 2020, to April 25th, 2020) and shows the remarkable increase in concentration of O_3 gas as a pollutant. Despite the complete lockdown over India during this given time frame, there has been enough emission of O_3 precursors from other sources such as stubble burning. The estimates of tropospheric O_3 concentration for May 2020 for Pune city, using OLS and RF Regressions, have been validated with May 2020 data. The results have provided a RMSE of 1.05 and 1.23 with R^2-statistics of 0.90 and 0.857 in training and testing phases for OLS and RMSE of 0.98 and MAE of 1.07 with R^2-statistics of 0.968 and 0.895 in training and testing phases of the RF. The outcome of this study has proven that O_3 gas concentrations in the atmosphere depends upon various other causative factors apart from the precursor gases. The study also shows that the remotely sensed Sentinel-5P datasets, supplemented with ground-based sensor data can help in time and cost saving estimation of O_3 concentrations in the troposphere with considerable accuracy.
4.	A Simplistic Approach to Bone Healing Simulation C Sen, J Prasad - Critical Reviews™ in Biomedical Engineering, 2022 **Abstract:** A simplistic computational approach to modelling and simulation of healing in long bone fractures is presented. In particular, an algorithm that could simulate the formation, maturation, and resorption of fracture callus is developed and validated. The simplicity of the approach lies in the fact that the algorithm uses only the applied load and a single constraint parameter for the entire simulation. The work hypothesizes bone healing as a comprehensive energy minimization process where mechanical stimulation is proposed as the primary precursor for the beginning of different stages (i.e., callus formation, mineralization, and resorption). As such, the hypothesis is derived from the second law of thermodynamics which states that the energy of a closed system should be minimum at equilibrium. Alternatively, each stage of healing bone healing may be termed a state of homeostasis. The validation is done through a multi-material, time-based simulation of bone healing in a damaged tibia. The simulation uses a cross-section-based finite element model and an advanced version of an already validated structural optimization algorithm. The optimization objective is to minimize overall strain energy for the entire process, subject to a polar first moment of mass constraint. The simulation results show different stages of healing, where the algorithm generates a callus geometry similar to those observed experimentally. Eventually, a geometry similar to that in an intact cross-section is achieved by resorption of the callus from the unwanted sites.
5.	A Survey on Evaluating the Quality of Autonomic Internet of Things Applications K Fizza, A Banerjee, PP Jayaraman, N Auluck.. - IEEE Communications Surveys & Tutorials, 2022 **Abstract:** The rapid evolution of the Internet of Things (IoT) facilitates the development of IoT applications in domains such as manufacturing, smart cities, retail, agriculture, etc. Such IoT applications collect data, analyze, and extract insightful information to enable decision-making and actuation. There is an unprecedented growth of IoT applications that automate decision-making and actuation without requiring human intervention, which we term autonomic IoT applications. The increasing scale of such applications necessitates holistic measurement and evaluation of application quality. Existing literature has evaluated quality from an end-user

	perspective, which may be unsuitable when dealing with the complexity of modern IoT applications, especially when they are autonomic. In this paper, we refer to IoT application quality as the aggregate quantitative value of various IoT quality metrics measured at each stage of the autonomic IoT application life cycle. We present an in-depth survey of current state-of-the-art techniques and approaches for evaluating quality of IoT applications. In particular, we survey various definitions to identify the factors that contribute to understanding and evaluating quality in IoT. Furthermore, we present open issues and identify future research directions towards realizing fine-grained quality evaluation of IoT applications. We envision that the identified research directions will, in turn, enable real-time diagnostics of IoT applications and make them quality-aware. This survey can serve as the basis for designing and developing modern, resilient quality-aware autonomic IoT applications.
6.	Adaptive Feature Consolidation Network for Burst Super-Resolution N Mehta, A Dudhane, S Murala, SW Zamir, S Khan, FS Khan - IEEE Computer Society Conference on Computer Vision and Pattern Recognition Workshops, 2022 **Abstract:** Modern digital cameras generally count on image signal processing (ISP) pipelines for producing naturalistic RGB images. Nevertheless, in comparison to DSLR cameras, low-quality images are generally output from portable mobile devices due to their physical limitations. The synthesized low-quality images usually have multiple degradations - low-resolution owing to small camera sensors, mosaic patterns on account of camera filter array and subpixel shifts due to camera motion. Such degradation usually restrain the performance of single image super-resolution methodologies for retrieving high-resolution (HR) image from a single low-resolution (LR) image. Burst image super-resolution aims at restoring a photo-realistic HR image by capturing the abundant information from multiple LR images. Lately, the soaring popularity of burst photography has made multi-frame processing an attractive solution for overcoming the limitations of single image processing. In our work, we thus aim to propose a generic architecture, adaptive feature consolidation network (AFCNet) for multi-frame processing. To alleviate the challenge of effectively modelling the long-range dependency problem, that multi-frame approaches struggle to solve, we utilize encoder-decoder based transformer backbone which learns multi-scale local-global representations. We propose feature alignment module to align LR burst frame features. Further, the aligned features are fused and reconstructed by abridged pseudo-burst fusion module and adaptive group upsampling modules, respectively. Our proposed approach clearly outperforms the other existing state-of-the-art techniques on benchmark datasets. The experimental results illustrate the effectiveness and generality of our proposed framework in upgrading the visual quality of HR images.
7.	Alcohols as alternative fuels in compression ignition engines for sustainable transportation: a review TK Sahu, PC Shukla, G Belgiorno, RK Maurya - Energy Sources, Part A: Recovery, Utilization, and Environmental Effects, 2022 **Abstract:** Alcohol fuels, primarily ethanol and methanol, have emerged as one of the important alternatives for sustainable transportation and power generation applications, due to the overall lower carbon dioxide (CO_2) emissions. The higher octane number of alcohol makes it suitable for spark ignition (SI) engines while lower blend ratios can be used for compression ignition (CI) engines as well. Since significant work and exploration have already been performed for the application of alcohol in SI engines, the present study is primarily focused on alcohol utilization

	in CI engines. This review majorly consists of three parts: first, a discussion on the physical and chemical properties of ethanol and methanol from the fuel perspective, second, combustion, and engine performance of CI engines fueled with alcohol and lastly, emissions characterization of alcohol as fuel. A summary of this review is provided which highlights the potential of alcohol utilization in the form of blend or under dual-fuel combustion modes, as well as neat alcohol fueled CI engine. Alcohol-fueled CI engine improves the soot-NOx trade-off characteristic in comparison to conventional diesel combustion, this fuel could be an enabler to meet future emissions regulations. Overall lower CO_2 emissions (up to 15% lower compared to diesel) by utilizing alcohol as fuel make it suitable for sustainable transportation.
8.	Algorithms for maximum internal spanning tree problem for some graph classes G Sharma, A Pandey, MC Wigal - Journal of Combinatorial Optimization, 2022 **Abstract:** For a given graph G, a maximum internal spanning tree of G is a spanning tree of G with maximum number of internal vertices. The Maximum Internal Spanning Tree (MIST) problem is to find a maximum internal spanning tree of the given graph. The MIST problem is a generalization of the Hamiltonian path problem. Since the Hamiltonian path problem is NP-hard, even for bipartite and chordal graphs, two important subclasses of graphs, the MIST problem also remains NP-hard for these graph classes. In this paper, we propose linear-time algorithms to compute a maximum internal spanning tree of cographs, block graphs, cactus graphs, chain graphs and bipartite permutation graphs. The optimal path cover problem, which asks to find a path cover of the given graph with maximum number of edges, is also a well studied problem. In this paper, we also study the relationship between the number of internal vertices in maximum internal spanning tree and number of edges in optimal path cover for the special graph classes mentioned above.
9.	An artificial neural network tool to support the decision making of designers for environmentally conscious product development PK Singh, P Sarkar - Expert Systems with Applications, 2022 **Abstract:** The consideration of sustainability aspects in initial stages of product development is understood as an effective approach to plan a sustainable product life cycle. It can be achieved by integrating the sustainability considerations into decision making of companies in early design phases. This study aims to develop an Artificial Intelligence (AI) tool that can assist the designers in their decision making to choose environmentally benign design parameters of products. The proposed tool is based on an Artificial Neural Network (ANN) model which takes the life cycle design parameters (viz. size of product, density of material, manufacturing process, transport mode and recyclability) as inputs and provides the corresponding outputs in terms of 'carbon footprint' and 'life cycle cost' of a product. These outputs assist the designers to realize the trade-off between the environmental load and cost effectiveness of a design alternative. Thus, it enables the decision making of companies to select a more sustainable design. A Graphical User Interface (GUI) is developed for the AI tool so that the designers can efficiently use this tool. The results predicted by the proposed tool are compared with the results obtained through the life cycle assessment carried out by using GaBi 9.2. The comparison shows that the results predicted by the tool have a reasonable accuracy of more than 90% which is significant, especially in the design stages of environmentally conscious product development. Also, the time efficiency of the tool to compute the environmental impact was compared with that of GaBi 9.2 by using a T-test. Results showed that the time efficiency of the proposed AI tool is significantly

	higher than that of GaBi 9.2.
10.	Analysis and Measurement of Non-Intrinsic Differential-Mode Noise in a SiC Inverter Fed Drive and Its Attenuation Using a Passive Sinusoidal Output EMI Filter M Kumar, J Kalaiselvi - IEEE Transactions on Energy Conversion, 2022 **Abstract:** The analysis, measurement, and attenuation of non-intrinsic differential-mode (NDM) and common-mode (CM) noise in an induction motor (IM) drive are discussed in this paper. In a voltage source inverter (VSI) fed drive, the NDM noise is caused by the excitation of the CM capacitance paths by the line to ground voltage. A measurement method at the input side of IM is proposed to separate intrinsic differential-mode (IDM), NDM, and CM noise from the total line current. It is substantiated that the NDM noise constitutes a significant portion of the measured DM noise. Hence, a passive sinusoidal output electromagnetic interference (EMI) filter (PSOEF) is presented to attenuate the NDM and CM noise. PSOEF is designed using line inductor & capacitor with the same resonance frequency to attenuate the NDM and CM noise. PSOEF has an advantage of reduced size and number of CM components as compared to conventional sinusoidal output EMI filter (CSOEF). The designed PSOEF is presented with space vector pulse width modulation (PWM) and CM voltage reduction PWM to analyze the attenuation performance, circulating current, and filter loss. The proposed measurement method and the design of PSOEF are experimentally validated on a SiC VSI switching at 200 kHz.
11.	Analysis of Common-Mode Noise and Mixed-Mode Differential-Mode Noise in Dual Active Bridge Converter B Dwiza, K Jayaraman, NBY Gorla, J Pou - IEEE Journal of Emerging and Selected Topics in Power Electronics, 2022 **Abstract:** The dual active bridge (DAB) converter is one of the widely explored topologies in recent years due to its remarkable features, such as inherent soft-switching characteristics, galvanic isolation, and high power density. However, the conducted electromagnetic interference (EMI) analysis of the DAB converter is seldom reported. In this paper, the common-mode (CM) and the differential-mode (DM) equivalent circuits of the isolated DAB converter are presented to understand the propagation mechanisms of the conducted EMI noise in the converter. In particular, the mixed-mode DM (MMDM) noise component of the DM noise is quantified for the DAB converter. Further, an experimental measurement method based on an external impedance-matched circuit is proposed to quantify the DM current due to the capacitive coupling between the primary and secondary windings of the transformer. The quantified MMDM noise and the DM noise through the transformer are estimated using the proposed equivalent circuits in MATLAB-Simulink and validated experimentally on a prototype DAB converter.
12.	Automatic Pasteurized Formula Milk Preparation Machine with Automatic Sterilized Containers AN Mallick, M Kumar, A Chander, R Kumar, K Arora, AK Sahni - 44th Annual International Conference of the IEEE Engineering in Medicine & Biology Society (EMBC), 2022 **Abstract:** Children are the future of our generation, so reducing child mortality is very critical in developing countries. There are lots of asserting factors of child mortality but malnutrition is one of the prominent factors. Medically, it has been proven that breastfeeding is one of the sources of nutrients and it is being always appreciated to have mothers' milk to a child in the early days. However, with the increasing participation of women in the workforce, the child care load on breastfeeding mothers is very high. This forces many of them to take long career breaks. Here, in

	this paper, we have an automatic formula milk dispensing unit that will be used in Neonatal Intensive Care Units (NICUs) and for breastfeeding mothers at home. The device has inbuilt sterilization and pasteurization units that would maintain the overall hygiene and sterilization of baby milk bottles. Currently, the device has a few buttons through which we can control the functionality of the device.
13.	Benchmarking PES-Learn's machine learning models predicting accurate potential energy surface for quantum scattering A Kushwaha, TJ Dhilip Kumar - International Journal of Quantum Chemistry, 2022 **Abstract:** Machine learning (ML) models, neural networks, and Gaussian processes have been used to predict the potential energy surface taking C_2-He (both static and dynamic scenario) and NCCN-He collision systems. The surface is restricted to ∽125 points where traditional spline becomes inefficacious. Quantum dynamics is performed by solving close-coupling equation to compute cross sections benchmarking the performance of the ML models. The current study forms a basis for any future investigation of larger molecules where conventional fitting fails due to sparser *ab initio* points and cuts down the computational time without compromising on the quality of the surface.
14.	BHT-NoC: Blaming Hardware Trojans in NoC Routers B Bisht, S Das - IEEE Design & Test, 2022 **Abstract:** Due to the cost and complexity of current multicore CPUs, chipmakers rely heavily on third-party IPs. A hostile IP or hardware Trojan (HT) on the Network-on-Chip (NoC) can degrade or leak packets. Several ways to identify HT in NoCs have been presented, but they are not robust. In this work, we propose the Blaming Hardware Trojan (BHT), which causes false positive HTs by exploiting current security features to decrease system performance. The proposed BHT attack can reduce affected router performance by 36.39%, and overall performance by 9.79%. The proposed countermeasure can recover it by losing only 2.6% performance.
15.	Cattle Collar: An End-to-End Multi-Model Framework for Cattle Monitoring G Singhal, P Choudhary, V Abhishek, S Sweety… N Goyal - IEEE 5th International Conference on Multimedia Information Processing and Retrieval (MIPR), 2022 **Abstract:** Individual cattle behaviour monitoring is a promising way of improving cattle farm management by detecting health issues and anomalies in behaviour patterns. Ac-celerometer sensors are non-invasive, low-cost devices that track daily activities and behaviour. For this, a hardware setup is attached to the neck collar of the cow to record its behaviour. We proposed an efficient data labelling method to classify simultaneously occurring activities with a single inertial sensor and a temperature sensor. Then a Machine Learning (ML) model is trained to predict the cattle activ-ities based on different time and frequency domain-based statistical features. The proposed method shows an accu-racy of 86% for Random Forest classifier. The behavioural analysis of an individual cow is sent to the user interface. The application provides visual data representation to mon-itor multiple cows daily and weekly.
16.	Cellular experiments to study the inhibition of c-Myc/MAX heterodimerization A Singh, S Sharma, P Kumar, N Garg - Methods in Enzymology, 2022 **Abstract:** The c-Myc oncogene is a master regulator of cancer cell metabolism, which controls a

	variety of pathways, including cell proliferation, cell cycle, apoptosis, and epigenetics. Belonging to the bHLH family of transcription factors, c-Myc forms a heterodimeric complex with another bHLH family protein MAX. c-Myc deregulation is reported in most cancers. This heterodimeric complex is a potent transcription factor that controls the expression of the target gene by binding to the *E*-box sequence and thereby controlling cancer cell proliferation. c-Myc in isolation has a partially folded structure and cannot carry the transcription. However, its heterodimerization provides the ability to bind DNA and carry out the regulatory function. Therefore, heterodimerization of c-Myc and Max is of great interest for cancers, and it has always been considered a target for cancer therapy. This book chapter will present a detailed protocol of cellular experiments employed to validate the in vitro potency of c-Myc inhibitor candidates to search for a novel c-Myc-targeted neoplastic drug.
17.	Cloud Removal in Satellite Imagery Using Adversarial Network and RGB-Optical Data Fusion S Ghildiyal, N Goel, M Saini - IEEE 5th International Conference on Multimedia Information Processing and Retrieval (MIPR), 2022 **Abstract:** Many earth observation activities rely on optical remote sensing data. The optical remote sensing imagery is ex-ploited in various applications like farmland monitoring, land use, land cover, 3D city models, vegetation growth, and disaster mitigation. Despite all, cloud cover significantly impacts on spatial and temporal accessibility of the earth observation. Since the first observation, it has been one persistent difficulty for optical remote sensing. For decades, researchers have been studying to remove clouds from optical images. The procedure of clearing the clouds becomes more difficult as they thicken. In such instances, it is customary to reconstruct utilizing additional images such as synthetic aperture radar (SAR) or near-infrared (NIR). In this paper, we propose a two-stage architecture-based cloud removal framework. The first stage of our network translates SAR and optical cloudy images to synthetic optical (RGB) image using the conditional Generative Adversarial Network (cGAN) and the second stage reconstructs the cloud-free image by fusing the synthetic optical (RGB) and cloudy optical image. The network was tested on the real cloudy images and the proposed method was compared with the state-of-the-art models and showed better results for cloud removal.
18.	Community Pool Model for Active-Hour Appliance Management: A Multi-Round ADMM Approach S Dash, R Sodhi, B Sodhi - IEEE Transactions on Smart Grid, 2022 **Abstract:** This paper proposes a decentralised pool-based local market model for a small energy community, intended to operate in parallel with an existing energy market, to manage the unscheduled active-hour (AH) appliances without violating the day-ahead nodal price of the community. The paper defines and targets this specific class of appliances with a two-stage iterative model. Stage-I calculates tentative AH sellers' schedule and the clearing price to cater the unscheduled AH buyers' needs. After getting the consensus from the AH sellers, Stage-II clears the pool. In every iteration, multiple rounds of information exchange ensure the maximisation of community-wide social-welfare in the binary-controlled AH resources' pool. The proposal is tested on the MATLAB platform with Gurobi solver using the Pecan-street's NewYork dataset, and reveals that the application of the proposed model has a superior appliance management performance in a stringent demand response scenario.
19.	Comparative Analysis of Prior Knowledge-Based Machine Learning Metamodels for Modeling Hybrid Copper–Graphene On-Chip Interconnects

	S Kushwaha, N Soleimani, F Treviso, R Kumar.. R Sharma - IEEE Transactions on Electromagnetic Compatibility, 2022 **Abstract:** In this article, machine learning (ML) metamodels have been developed in order to predict the per-unit-length parameters of hybrid copper–graphene on-chip interconnects based on their structural geometry and layout. ML metamodels within the context of this article include artificial neural networks, support vector machines (SVMs), and least-square SVMs. The salient feature of all these ML metamodels is that they exploit the prior knowledge of the p.u.l. parameters of the interconnects obtained from cheap empirical models to reduce the number of expensive full-wave electromagnetic (EM) simulations required to extract the training data. Thus, the proposed ML metamodels are referred to as prior knowledge-based machine learning (PKBML) metamodels. The PKBML metamodels offer the same accuracy as conventional ML metamodels trained exclusively by full-wave EM solver data, but at the expense of far smaller training time costs. In this article, detailed comparative analysis of the proposed PKBML metamodels have been performed using multiple numerical examples.
20.	Critical rates of climate warming and abrupt collapse of ecosystems T Kaur, PS Dutta - Proceedings of the Royal Society A: Mathematical, Physical and Engineering Sciences, 2022 **Abstract:** In the age of climate warming, comprehension of ecosystems' future is one of the pressing challenges to humanity. While most studies on climate warming focus on the 'magnitude of change' of the Earth's temperature, the 'rate' at which it is increasing cannot be ruled out. Rapid warming has already caused sudden ecosystem transitions at numerous biodiversity hot spots; a mechanistic understanding of such transitions is crucial. Here, we study a slow–fast consumer–resource ecosystem interacting in rapid warming scenarios. Employing geometric singular perturbation theory, we find that while a gradual change in mean temperature may accord population persistence, a critical warming rate can drive the resource's sudden collapse, termed a warming-induced abrupt transition. This further triggers the bottom-up effect, resulting in the extinction of the consumer. The difference between the optimum temperature of the resource's growth rate and the habitat temperature is crucial in deciding the critical rate of warming. Consequently, species inhabiting extreme temperature regions are more susceptible to warming-induced collapse than those within intermediate temperature ranges. We find that stochastic fluctuations in the system can advance warming-induced transitions, and the efficacy of generic early warning signals to anticipate sudden transitions is challenged.
21.	Cross Layer MAC Protocol for a Peer Conscious Opportunistic Network Coded Cooperation System S Bhattacharyya, P Kumar, S Darshi, S Agarwal.. - IEEE Transactions on Mobile Computing, 2022 **Abstract:** This paper presents a peer conscious opportunistic network coded cooperation (PC-O-NCC) system that exploits multi-user diversity (MUD) gain in a simple network coded cooperation (NCC) based network. It prioritizes sources with better channel conditions by granting them earlier access than the other competing nodes unlike the prevalent time division multiple access (TDMA) technique used widely in any NCC network. This improves the outage performance of the overall system. To prioritise sources with better channel conditions, a novel timer-based MAC protocol is proposed. The proposed protocol is designed such that it aims to

	reduce collisions by taking the network load into account along with channel conditions while generating the timer values. It also minimizes the power consumption in performing clear channel assessment (CCA) by sources which is a costly affair for battery-operated devices. The simulation results show that the proposed algorithm improves the outage performance while keeping the latency to a minimum value. The improvement in the outage performance can prove to be important in taking key decisions which becomes crucial in disaster management, drone assisted scenarios or intelligent transportation systems.
22.	Dynamic mode decomposition analysis and fluid-mechanical aspects of viscoelastic fluid flows past a cylinder in laminar vortex shedding regime F Hamid, C Sasmal, R Chhabra - Physics of Fluids, 2022 **Abstract:** This study presents an extensive numerical investigation to understand the effect of fluid viscoelasticity on the flow dynamics past a stationary cylinder in the laminar vortex shedding regime. In particular, for the first time, this study presents a detailed analysis of how the fluid viscoelasticity influences the coherent flow structures in this benchmark problem using the dynamic mode decomposition (DMD) technique, which is considered to be one of the widely used reduced order modeling (ROM) technique in the domain of fluidmechanics. We show that this technique can successfully identify the low-rank fluid structures in terms of the spatiotemporal modes from the time-resolved vorticity field snapshots and capture the essential flow features by very few modes. Furthermore, we observe a significant difference in the amplitude and frequency associated with these modes for Newtonian and viscoelastic fluids otherwise under the same conditions. This, in turn, explains the differences seen in the flow dynamics between the two types of fluids in an unambiguous way, such as why the fluid viscoelasticity suppresses the vortex shedding phenomenon and decreases the energy associated with the velocity fluctuations in viscoelastic fluids than that in Newtonian fluids. However, before performing the DMD analysis, we also present a detailed discussion on the various fluid-mechanical aspects of this flow system, such as streamline patterns, vorticity fields, drag and lift forces acting on the cylinder, etc. This will ultimately set a reference platform for delineating the importance of the DMD analysis to get further insights into the flow physics.
23.	Effect of emotional intelligence and cognitive flexibility on entrepreneurial intention: mediating role of entrepreneurial self-efficacy A Mishra, P Singh - Journal of Entrepreneurship in Emerging Economies, 2022 **Abstract:** Purpose Entrepreneurship is one of the significant drivers of economic growth, development and job generation in several countries worldwide. Realizing its significant contribution to the nation’s development, policymakers and educators have also drawn attention to fostering entrepreneurship among the youth. Researchers attempted to comprehend the dynamics and investigate the factors influencing entrepreneurial intention (EI). As is true for other abilities and response tendencies, individual differences exist for EI also. This study aims to explore the relationship of emotional intelligence (EIn) and cognitive flexibility (CF) with EI and mediating effect of entrepreneurial self-efficacy (ESE) in the relationship between CF, EIn and EI.

	Design/methodology/approach The cross-sectional survey was conducted to gather responses from 635 individuals aged 17–26 years (M = 19.2, SD = 1.49). The hypotheses were tested using correlation, regression and mediation analysis. Findings The findings indicated that EIn and CF were significantly and positively related to EI. Furthermore, ESE was found to be a partial mediator between EIn and EI and a full mediator between CF and EI. Research limitations/implications Results reflected the critical significance of ESE and implied that EI might be strengthened by intervening in ESE through various sources. Originality/value This study adds to the existing literature by incorporating less studied individual factors (EIn and CF) to better understand EI by explaining the mediation mechanism through ESE.
24.	Effect of microstructure on tool wear in micro-turning of wrought and selective laser melted Ti6Al4V J Airao, CK Nirala - Materials Letters, 2022 **Abstract:** Additively manufactured (AM) parts are not often suitable for direct application as they require post-processing to remove the surface imperfections. Moreover, AM parts have a different microstructure than conventionally fabricated parts. In this regard, this article presents a comparative analysis of the effect of microstructure on tool wear during micro-turning of conventionally manufactured and selective laser melting (SLM) or laser powder bed fusion (LPBF) fabricated Ti6Al4V. Primary tool wear mechanisms found are abrasion, adhesion, and built-up edge formation for both the materials. Moreover, edge chipping is found in the case of the LPBF Ti6Al4V attributed to their higher hardness than wrought Ti6Al4V. More tool wear for LPBF Ti6Al4V is primarily caused due to an instability of the β phase at a higher temperature. Alternatively, equiaxed grains of wrought Ti6Al4V show lesser tool wear due to a balanced hardness and yield strength compared to LPBF Ti6Al4V.
25.	Efficient Sensing of Selected Amino Acids as Biomarker by Green Phosphorene Monolayers: Smart Diagnosis of Viruses P Panigrahi, Y Pal, A Panigrahi, H Bae, H Lee, R Ahuja.. - Advanced Theory and Simulations, 2022 **Abstract:** Effective techniques for the detection of selected viruses detection of their amino acids (AAs) constituents are highly desired, especially in the present COVID pandemic. Motivated by this, we have used density functional theory (DFT) simulations to explore the potential applications of green phosphorene monolayer (GPM) as efficient nanobio-sensor. We have employed van der Waals induced calculations to study the ground-state geometries, binding

	strength, electronic structures, and charge transfer mechanism of pristine, vacancy-induced and metal-doped GPM to detect the selected AAs, such as glycine, proline and aspartic, in both aqueous and non-aqueous media. We find that the interactions of studied AAs are comparatively weak on pristine (−0.49 to −0.76 eV) and vacancy-induced GPM as compared to the metal-doped GPM (−0.62 to −1.22 eV). Among the considered dopants, Ag-doping enhances the binding of AAs to the GPM stronger than the others. In addition to appropriate binding energies, significant charge transfers coupled with measurable changes in the electronic properties further authenticate the potential of GPM. Boltzmann thermodynamic analysis have been used to study the sensing mechanism under varied conditions of temperatures and pressure for the practical applications. Our findings signify the potential of GPM based sensors towards efficient detection of the selected AAs.
26.	Electrical Resistance Tomography (ERT) applied to Epoxy composites R Phartiyal, PK Agnihotri, N Gupta - IEEE 4th International Conference on Dielectrics (ICD), 2022 **Abstract:** Polymer composites like epoxy are widely used in high performance engineering applications requiring electrical insulation and/or mechanical strength and resistance to cyclic stresses. Over time, multi-stress aging can result in progressive degradation of the polymer. The current work studies the possibility of damage detection in epoxy through electrical resistance tomography. In electrical resistance tomography (ERT), current is injected at known points in the sample, and the resultant potential difference between given points is measured. For this purpose, an array of electrodes is placed along the boundary of the sample. Further, this technique requires the conductivity of the polymer to be increased to measurable values, and this is done by incorporating carbon-reinforced fibers into the matrix to form a Carbon Fiber Reinforced Polymer (CFRP). A finite element method (FEM) based model is developed to model the electrical resistance tomography measurements in epoxy-based CFRP in the presence of simulated defects. The ERT measurements are observed to be sensitive to the presence of defects.
27.	Electro-thermal modeling and reliability analysis of Cu–carbon hybrid interconnects for beyond-CMOS computing B Kumari, R Sharma, M Sahoo - Applied Physics Letters, 2022 **Abstract:** A Cu–carbon hybrid interconnect was recently proposed as an alternate interconnect structure for future VLSI applications because of its superior electrical performance over its counterparts. This study focuses on the electro-thermal aspects of Cu–carbon hybrid interconnects to be adopted as a potential replacement of copper as the back-end-of-line (BEOL) interconnect material. Cu–carbon hybrid shows promise in terms of electro-thermal efficiency when compared to copper as well as other suggested hybrid materials. The maximum temperature attained by the Cu–carbon hybrid interconnect is less than copper by 16%, and its mean time to failure is improved by 96%. Uniform distribution of heat can be observed in the Cu–carbon hybrid BEOL in addition to low temperature rise as compared to the copper based BEOL. These analyses strengthen the claim of Cu–carbon hybrid interconnects to be a worthier possibility for electro-thermal efficient nanoscale systems.
28.	Energy-and-delay-aware scheduling and load balancing in vehicular fog networks V Sethi, S Pal, A Vyas, S Jain, K Naik - Telecommunication Systems, 2022

	Abstract: Roadside units (RSUs) play an important role in the request fulfillment of vehicles. In rural areas, RSUs are powered by renewable energy sources like solar energy. Hence, the request fulfillment of vehicles must be done in such a way that the energy consumption across RSUs is minimized. The requests are categorized into traditional application (low computation) requests and smart application (high computation) requests. To avoid excessive computation at RSUs, low computation requests are scheduled across RSUs while high computation requests are scheduled across fog servers for processing. In this paper, we propose an online **e**nergy-**e**fficient **I**nter-**R**SU **S**cheduling **A**lgorithm (ee-IRSA) and a **d**istributed **A**nt **C**olony **O**ptimization-based **L**oad balancing technique (d-ACOL) for optimizing the request fulfillment of traditional and smart application requests, respectively. ee-IRSA ensures minimum and uniform energy consumption across RSUs while d-ACOL ensures minimum queue waiting time of requests across fog servers. In addition, a second-price auction game-based relay vehicle selection technique is proposed which further minimizes the energy consumption of RSUs. Simulation results show that ee-IRSA with relay vehicle selection reduces the energy consumption by 33%33%, and d-ACOL reduces the queue waiting time by an average of 48%48% as compared to other load balancing techniques.
29.	Enhancing aging resistance of glass fiber/epoxy composites using carbon nanotubes A Chauhan, HS Bedi, PK Agnihotri - Materials Chemistry and Physics, 2022 **Abstract:** An experimental investigation is carried out to examine the effectiveness of carbon nanotubes (CNT) in minimizing the environmental assisted degradation of glass fiber/epoxy composites (GFRP). To this end, CNT modified epoxy is used to fabricate glass fiber/epoxy hybrid composites (CNTGFRP). Experimental results show that the addition of 1 wt% of CNT in conventional GFRP increases the interlaminar shear strength (ILSS) by 36% and decreases the volumetric electrical resistance by 46%. Effect of environmental factors is studied by exposing composite samples to 500 h of accelerated weathering cycle. The exposure to aging cycle not only changes the colour and microstructure, it also increases the ILSS and electrical resistance of GFRP and CNTGFRP composite samples. These changes are primarily attributed to the loss of polymer matrix and improved crosslinking in composites caused by moisture, temperature and UV rays during the aging process. It is recorded that while the deformation in unaged composites is of ductile nature, the aged samples show fiber dominated brittle behavior. Finally, it is shown that the incorporation of CNT in the matrix not only ensures structural integrity but also reduces environmental assisted degradation of conventional glass fiber/epoxy composites. **Graphical Abstract:** 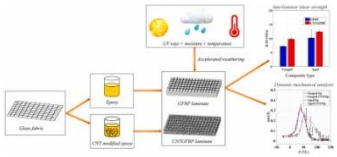
30.	Experimental and numerical verification of anomalous screening theory in granular matter C Mondal, M Moshe, I Procaccia, S Roy, J Shang… - Chaos, Solitons & Fractals, 2022 **Abstract:** The concept of mechanical screening is widely applied in solid-state systems.

	Examples include nucleation of defects in crystalline materials, scars and pleats in curved crystals, wrinkles in strongly confined thin sheets, and cell-rearrangements in biological tissue. Available theories of such screening usually contain a crucial ingredient, which is the existence of an ordered reference state, with respect to which screening elements nucleate to release stresses. In contradistinction, amorphous materials in which a unique reference state does not exist, nevertheless exhibits plastic events that act as screening geometric charges with significant implications on the mechanical response. In a recent paper [Phys. Rev. E **104**, 024904] it was proposed that mechanical strains in amorphous solids can be either weakly or strongly screened by the formation of low or high density of plastic events. At low densities the screening effect is reminiscent of the role of dipoles in dielectrics, in only renormalizing the elastic moduli. The effect of high density screening has no immediate electrostatic analog and is expected to change qualitatively the mechanical response, as seen for example in the displacement field. On the basis of experiments and simulations, we show that in granular matter, strong screening results in significant deviation from elasticity theory. The theoretical analysis, which accounts for an emergent inherent length scale, the experimental measurements and the numerical simulations of frictional granular amorphous assemblies are in agreement with each other, and provide a strong support for the novel continuum theory.
31.	Experimental Investigation and Performance Optimization during Machining of Hastelloy C-276 Using Green Lubricants G Singh, V Aggarwal, S Singh, B Singh, S Sharma.. – Materials, 2022 **Abstract:** Smart manufacturing is the demand of industry 4.0, in which the mass production of difficult-to-cut materials is of great concern to fulfil the goal of sustainable machining. Presently, the machining of superalloy is of upmost interest because of its wide application. However, the limited data on the turning of Hastelloy C-276 highlights its challenges during processing. Hence, the machining performance of superalloy considering surface quality, thermal aspects and chip reduction coefficient was examined with minimum quantity lubrication of several oils to address the sustainable development goal (SDG-12). The output responses were optimized through response surface methodology along with analysis of variance. The research exhibited that the output responses were dominated by cutting speed and feed rate having a percentage benefaction of 24.26% and 60%, respectively, whilst the depth of cut and lubricant type have an influence of 10–12%. No major difference in temperature range was reported during the different lubrication conditions. However, a substantial variation in surface roughness and the chip reduction coefficient was revealed. The percentage error evaluated in surface roughness, temperature and chip reduction coefficient was less than 5%, along with an overall desirability of 0.88, describing the usefulness of the model used. The SEM micrograph indicated a loss of coating, nose and flank wear during all lubrication conditions. Lastly, incorporating a circular economy has reduced the economic, ecological and environmental burden.
32.	Explainable machine learning aided optimization of masonry infilled reinforced concrete frames I Latif, A Banerjee, M Surana – Structures, 2022 **Abstract:** Machine learning has become a powerful tool in structural and earthquake engineering to accurately predict structural design parameters; however, these complex algorithms are highly inexplainable. In this work, two machine learning algorithms, i.e., Neural Network and eXtreme Gradient Boosting are used to predict the fundamental period of vibration of masonry infilled reinforced concrete frames. The input parameters considered for predicting the fundamental

	period of vibration of masonry infilled reinforced concrete frames are the number of storeys, opening ratio, span length, number of spans, and masonry wall stiffness. The model predictions are explained globally and locally, using the partial dependence plots, the accumulated local effects, and the game theory-based approach of Shapely values. The performance of the trained machine learning models is compared with expressions existing in the literature and building codes to predict the fundamental period of vibration of masonry infilled reinforced concrete frames. Finally, the trained machine learning models and the existing equation in the literature are used as surrogates to optimize the opening ratio and masonry wall stiffness of buildings present in the database using the genetic algorithm approach. Therefore, the adopted methodology results in a new database of buildings created together by machine learning and optimization algorithms, and the methodology can be used to optimize the opening ratio and masonry wall stiffness to achieve a targeted fundamental period. The dashboard for predicting and optimizing the fundamental period using the trained machine learning models are also developed as a part of this study.
33.	Exploring AZ31B magnesium alloy for innovative micro products by reverse-μEDM H Kishore, CK Nirala, A Agrawal – Materials Letters, 2022 **Abstract:** Fabrication of complex and filigree magnesium alloy 3D-medical implants is very difficult by conventional processes. The present work examines the feasibility of fabricating arrayed microstructures (protrusions) of magnesium AZ31B Mg alloy in unconventional profiles. For this, Reverse-μEDM integrated with laser beam micromachining (LBμM), as a new hybrid technology, is employed. A capacitance of 10 nF, a voltage of 110 V and a feed rate of 10 μm/min for Reverse-μEDM led to better machining responses in terms of materials removal rate, tool wear, and avg. surface roughness compared to other parametric settings. Considering the importance of the biocompatibility of materials, the surface integrity of the fabricated microstructures is also analyzed.
34.	First-principles study of two-dimensional C-silicyne nanosheet as a promising anode material for rechargeable Li-ion batteries N Duhan, TJD Kumar - Physical Chemistry Chemical Physics, 2022 **Abstract:** Li-ion batteries are one of the sustainable alternatives to meet the growing energy demands of an increasing population. However, finding a suitable negative electrode is key for improving battery performance. In the present work, first principles-based investigations are carried out to explore the capability of a planar 2D C-silicyne nanosheet – which is a Si analogue of α-graphyne having –C≡C– substitution – as an anode for improving the performance of Li-ion batteries. Thermally and dynamically stable C-silicyne sheets exhibit a metallic nature as inferred from the density of states studies. The average adsorption energies for sequential adsorption of the Li atom over the monolayer range from −1.35 to −0.46 eV, implying favourable interactions between the monolayer and the Li atom which indicate that during the lithiation process, clustering amongst the metal atoms is not preferred. The energy barrier for the migration of Li-ions is 0.21 eV, indicating an active charge/discharge process. A high storage capacity of 836.07 mA h g^{-1} and a working potential of 0.60 V is obtained. A negligible amount of volume change of the C-silicyne monolayer after full lithiation is observed which implies good cyclability. All these outcomes imply that C-silicyne nanosheets are a potential anode material for next-generation LIBs.

	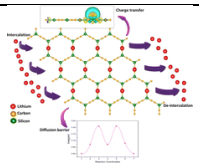
35.	Generating high-energy densities by sidelobe suppression in the far-field of phase-locked lasers V Dev, ANK Reddy, V Pal - Journal of the Optical Society of America B: Optical Physics, 2022 **Abstract:** Laser beams with high-energy densities are desired for both fundamental research and applied applications. We present a numerical study on the generation of high-energy densities by sidelobe suppression in the far-field intensity distribution of phase-locked lasers. The method relies on modifying the combined field distribution of phase-locked lasers to obtain uniform amplitude and phase distributions in a near-field plane, which enables the formation of a high-energy density main central lobe (zeroth order) in the far field. The method is applied to various one-dimensional (1D) and two-dimensional (2D) array geometries, such as square, triangular, Kagome, random, and 1D ring. The results show that for in-phase-locked lasers in 2D array geometries, the diffraction efficiency of the high-energy density region (zeroth-order lobe) can be increased in the range of 90%–95%. For in-phase-locked lasers in a 1D ring array, the maximum diffraction is found to be ~75%~75%. Further, the effects of the range of phase locking, system size, as well as topological defects are examined on diffraction efficiency. The method is also applied to an out-of-phase-locked laser in the square array, and a high-energy density output beam is obtained.
36.	Genome-wide DNA hypermethylation opposes healing in patients with chronic wounds by impairing epithelial-mesenchymal transition K Singh, Y Rustagi, AS Abouhashem, S Tabsum.. D Pal.. – The Journal of clinical investigation, 2022 **Abstract:** An extreme chronic wound tissue microenvironment causes epigenetic gene silencing. An unbiased whole-genome methylome was studied in the wound-edge tissue of patients with chronic wounds. A total of 4,689 differentially methylated regions (DMRs) were identified in chronic wound-edge skin compared with unwounded human skin. Hypermethylation was more frequently observed (3,661 DMRs) in the chronic wound-edge tissue compared with hypomethylation (1,028 DMRs). Twenty-six hypermethylated DMRs were involved in epithelial-mesenchymal transition (EMT). Bisulfite sequencing validated hypermethylation of a predicted specific upstream regulator TP53. RNA-Seq analysis was performed to qualify findings from methylome analysis. Analysis of the downregulated genes identified the *TP53* signaling pathway as being significantly silenced. Direct comparison of hypermethylation and downregulated genes identified 4 genes, *ADAM17*, *NOTCH*, *TWIST1*, and *SMURF1*, that functionally represent the EMT pathway. Single-cell RNA-Seq studies revealed that these effects on gene expression were limited to the keratinocyte cell compartment. Experimental murine studies established that tissue ischemia potently induces wound-edge gene methylation and that 5′-azacytidine, inhibitor of methylation, improved wound closure. To specifically address the significance of *TP53* methylation, keratinocyte-specific editing of *TP53* methylation at the wound edge was achieved by a tissue nanotransfection-based CRISPR/dCas9 approach. This work identified that reversal of methylation-dependent keratinocyte gene silencing represents a productive therapeutic strategy to improve wound

	closure. **Graphical Abstract:** 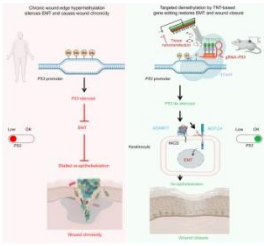
37.	Has COVID-19 intensified the oil price–exchange rate nexus? KB Chowdhury, B Garg - Economic Analysis and Policy, 2022 **Abstract:** This paper extends the existing empirical literature by investigating whether the COVID-19 crisis has strengthened the dynamic relationships between oil price and exchange rate. We find significant breaks in the relationships wherein a common break is detected around the COVID-19 outbreak period. Of note, the interactions between the two markets intensified since the outbreak of the COVID-19 pandemic. Overall, our findings imply that the investors and policymakers are taking stock of the valuable information from the unanticipated occurrence of the COVID-19 pandemic. Thus, diversification in the form of portfolio switches towards foreign currency-denominated assets may be effective in the case of a depreciation of the domestic currency.
38.	High throughput virtual screening (HTVS) of peptide library: Technological advancement in ligand discovery NM Tripathi, A Bandyopadhyay - European Journal of Medicinal Chemistry, 2022 **Abstract:** High-throughput virtual screening (HTVS) is a leading biopharmaceutical technology that employs computational algorithms to uncover biologically active compounds from large-scale collections of chemical compound libraries. In addition, this method often leverages the precedence of screening focused libraries for assessing their binding affinities and improving physicochemical properties. Usually, developing a drug sometimes takes ages, and lessons are learnt from FDA-approved drugs. This screening strategy saves resources and time compared to laboratory testing in certain stages of drug discovery. Yet in-silico investigations remain challenging in some cases of drug discovery. For the last few decades, peptide-based drug discoveries have received remarkable momentum for several advantages over small molecules. Therefore, developing a high-fidelity HTVS platform for chemically versatile peptide libraries is highly desired. This review summarises the modern and frequently appreciated HTVS strategies for peptide libraries from 2011 to 2021. In addition, we focus on the software used for preparing peptide libraries, their screening techniques and shortcomings. An index of various HTVS methods reported here should assist researchers in identifying tools that could be beneficial for their peptide library screening projects. **Graphical Abstract:** This review delineates the scope of high-throughput virtual screening (HTVS) in peptide binder and drug discovery. It also discussed the software information for peptide library preparation and HTVS. The article concludes with a handful of examples of

	HTVS subjected to experimental validation. 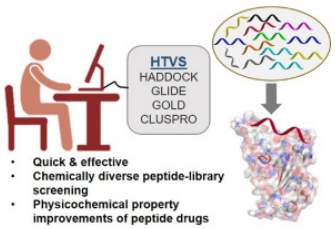
39.	Hybrid quantum-classical solution for electric vehicle charger placement problem PU Rao, B Sodhi - Soft Computing, 2022 **Abstract:** Building a dependable network of electric vehicle charging stations (EVCSs) requires satisfying the demands and constraints of EV owners, energy grids, and the entities that will own and operate the EVCSs. Thus, determining the optimal spatial placement of EVCS becomes essential for the success of EVs in a market. Time taken by classical computers to solve such combinatorial optimization problems increases exponentially with the size of the area, making them non-scalable. We propose a novel quantum-classical solution to solve this problem. A crucial idea of our approach is to move the more complex combinatorial optimization portion of the problem into a quantum algorithm. We show that our solution gives more than 500% improvement in speed compared to the state-of-the-art classical methods, thus making it well suited for scalability scenarios. For allowing independent verification of our results, we have shared all our software artefacts here: https://bit.ly/EVCS-Paper
40.	Hydrogen passivated β_{12}-borophene nanoribbon: A propitious one-dimensional metallic anode for sodium-ion rechargeable batteries S Choudhary, N Duhan, TJD Kumar - Applied Surface Science, 2022 **Abstract:** Synthesized borophene nanoribbons are the single-atom-thick self-assembly of light weight boron atoms separated by hexagonal hole arrays. In this current study, van der Waals corrected density functional theory have been employed to inspect the interaction of Na with both edge hydrogen passivated β12-borophene nanoribbon, based upon first-principles calculations. It is found that the six member ring site is favorable location for Na insertion. Gradual decrease in adsorption energies is observed with increasing Na concentration owing to the fact that the number of vacant sites on anchoring nanoribbon decreases and metal–metal electrostatic repulsion increases. The chemical stoichiometry of full sodiated nanoribbon corresponds to $B_{11}H_2Na_7$ with a maximum gravimetric capacity of 1551.65 $mAhg^{-1}$ without the sacrifice of Na mobility (diffusion barrier of 0.38 eV). Bader charge investigation reveals that 0.83|e| is transferred from Na atom, implying high electronic conductivity of $B_{33}H_6$ nanoribbon during the adsorption process. The average insertion potential is obtained as 0.66 V versus Na/Na+, lying into 0.1–1 V desirable anode potential range. Our study confirm that β12-borophene nanoribbon holds a great potential to act as a propitious negative electrode material for sodium-ion rechargeable batteries based on its structural, electronic and electrochemical properties. **Graphical Abstract:**

	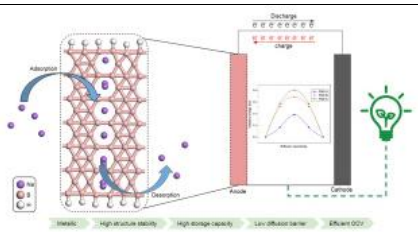
41.	Image inpainting via spatial projections SS Phutke, S Murala - Pattern Recognition, 2022 **Abstract:** Image inpainting is now-a-days sought after due to its wide variety of applications in the reconstruction of the corrupted image, occlusion removal, reflection removal, etc. Existing image inpainting approaches utilize different types of attention mechanisms to inpaint the image and produce visibly admirable results. These methods are more concerned at weighing the feature maps of the hole region with some weight from the non-hole region. But, due to the lack of spatial contextual correlation in the attention maps, the inpainted image may suffer from the inconsistencies among hole and non-hole regions. Transformer-based inpainting methods give significant results by capturing the relationship between the patches with a compromise of high computational complexity. In this context, we propose a novel spatial projection layer (SPL) without any attention mechanism to project the spatial contextual information in the hole region from non-hole regions for producing a spatially plausible inpainted image. The SPL is proposed mainly to focus on the non-hole spatial information in the high-level feature maps for filling the hole regions efficiently. Also, while training the network, we propose the use of edge loss with a Canny edge operator for image inpainting to focus on the relevant edges instead of noise contents. Analysis with the extensive experiments, ablation, and user study on the proposed architecture demonstrates the superiority over existing state-of-the-art methods for image inpainting. The code is available at: https://github.com/shrutiphutke/spatial_projection_inpainting.
42.	Impact of Fading on Association Probability in UAV-Enabled IoT Networks N Gupta, S Agarwal, D Mishra - IEEE Vehicular Technology Conference, 2022 **Abstract:** In an unmanned aerial vehicle (UAV)-enabled Inter-net of Thing (IoT) network, the transmission rate of an IoT node from the aerial base station (ABS) is determined by the signal-to-noise ratio (SNR). In general, the characterization of the ABS-to-node (A2N) channel is determined by its instantaneous SNR. The previous works reported in this direction have considered the average SNR. This study fills the gap in understanding how fading affects the network's performance. In this paper, we consider a UAV-enabled IoT network, where multiple ABSs are deployed to serve the IoT nodes. We model the A2N channel based on the instantaneous channel; we consider a generalized fading model, the Nakagami-m model for the A2N link, to provide a more generic analysis. Through analytical insights, we obtain the exact and closed-form approximate expression of the association probability of IoT node with the ABS and infer the capacity enhancement obtained by considering fading compared to the average SNR scenario. The average improvement in ergodic capacity is around 10% compared to the average fading scenario. Furthermore, the results show that considering fading is beneficial for low-altitude scenarios, as it provides a significant increase in the node association probability compared to the average fading scenario.

43.	Indentation size effect in steels with different carbon contents and microstructures SS Sarangi, A Lavakumar, PK Singh, PK Katiyar, RK Ray – Materials Science and Technology, 2022 **Abstract:** Indentation Size Effect (ISE) in steels having a wide spectrum of carbon (C) concentrations (wt-%) 0.002 (interstitial-free), 0.07 (microalloyed), 0.19 (low carbon), 0.32 (medium carbon), and 0.7 (high carbon), and microstructures were investigated using Vickers micro-hardness tester. A decrease in micro-hardness with increasing load, i.e. ISE, is observed in all the samples except microalloyed steel. The empirical relations, such as the Nix and Gao model, Minimum Resistance model, and Proportional Specimen Resistance (PSR) model, were used to determine the load-independent or true hardness values. Nix and Gao model was adopted to determine the plastically deformed zone (PDZ) size under the indenter and subsequently correlated with ISE in the materials. It is observed that ISE is absent when the PDZ size becomes comparable to or larger than the grain size of the material.
44.	Interaction of surface water waves with an elastic plate over an arbitrary bottom topography A Kaur, SC Martha - Archive of Applied Mechanics, 2022 **Abstract:** In the present paper, the problem involving the transformation of incident wave energy by floating elastic structure situated at a finite distance from an arbitrary bottom topography is studied. Here, both symmetric and asymmetric bottom profiles, which are arbitrary in nature, are considered . The successive steps are used to approximate the uneven bottom profile. The method of step approximation along with matched eigenfunction expansion is employed by which a system of linear algebraic equations is obtained and solved to determine the hydrodynamic quantities, namely transmission and reflection coefficients, plate deflection, strain and shear force on the plate. The present results are validated with the known results of literature for the case of rigid floating structure over the uniform finite depth as a particular case. The energy identity is obtained through Green integral theorem and is checked in towards the accuracy of present results. The effect of various structural and system parameters such as elastic plate length, angle of incidence, depth ratios, distance between the bottom topography and elastic plate on transmission and reflection coefficients, shear force and strain, plate deflection is investigated through different graphs and tables. This problem will give useful information to create the desirable tranquility zone near the seashore.
45.	Investigation of Tensile Properties of Different Infill Pattern Structures of 3D-Printed PLA Polymers: Analysis and Validation Using Finite Element Analysis in ANSYS S Ganeshkumar, SD Kumar, U Magarajan.. S Sharma.. - Materials, 2022 **Abstract:** The advancement of 3D-printing technology has ushered in a new era in the production of machine components, building materials, prototypes, and so on. In 3D-printing techniques, the infill reduces the amount of material used, thereby reducing the printing time and sustaining the aesthetics of the products. Infill patterns play a significant role in the property of the material. In this research, the mechanical properties of specimens are investigated for gyroid, rhombile, circular, truncated octahedron, and honeycomb infill structures (hexagonal). Additionally, the tensile properties of PLA 3D-printed objects concerning their infill pattern are demonstrated. The specimens were prepared with various infill patterns to determine the tensile properties. The fracture of the specimen was simulated and the maximum yield strengths for different infill structures and infill densities were determined. The results show the hexagonal

	pattern of infill holds remarkable mechanical properties compared with the other infill structures. Through the variation of infill density, the desired tensile strength of PLA can be obtained based on the applications and the optimal weight of the printed parts.
46.	Investigation of Water Evaporation Process at Air/Water Interface using Hofmeister Ions B Rana, DJ Fairhurst, KC Jena - Journal of the American Chemical Society, 2022 **Abstract:** Evaporation is an interfacial phenomenon in which a water molecule breaks the intermolecular hydrogen (H−) bonds and enters the vapor phase. However, a detailed demonstration of the role of interfacial water structure in the evaporation process is still lacking. Here, we purposefully perturb the H-bonding environment at the air/water interface by introducing kosmotropic (HPO_4^{-2}, SO_4^{-2}, and CO_3^{-2}) and chaotropic ions (NO_3^- and I^-) to determine their influence on the evaporation process. Using time-resolved interferometry on aqueous salt droplets, we found that kosmotropes reduce evaporation, whereas chaotropes accelerate the evaporation process, following the Hofmeister series: $HPO_4^{-2} < SO_4^{-2} < CO_3^{-2} < Cl^- < NO_3^- < I^-$. To extract deeper molecular-level insights into the observed Hofmeister trend in the evaporation rates, we investigated the air/water interface in the presence of ions using surface-specific sum frequency generation (SFG) vibrational spectroscopy. The SFG vibrational spectra reveal the significant impact of ions on the strength of the H-bonding environment and the orientation of free OH oscillators from ∼36.2 to 48.4° at the air/water interface, where both the effects follow the Hofmeister series. It is established that the slow evaporating water molecules experience a strong H-bonding environment with free OH oscillators tilted away from the surface normal in the presence of kosmotropes. In contrast, the fast evaporating water molecules experience a weak H-bonding environment with free OH oscillators tilted toward the surface normal in the presence of chaotropes at the air/water interface. Our experimental outcomes showcase the complex bonding environment of interfacial water molecules and their decisive role in the evaporation process. 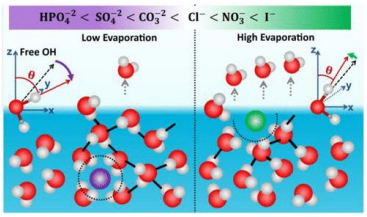
47.	Investigating the environmental impacts of coal mining using remote sensing and in situ measurements in Ruqigou Coalfield, China V Saini, J Li, Y Yang, J Li, B Wang, J Tan - Environmental Monitoring and Assessment, 2022 **Abstract:** China is the largest producer and consumer of coal in the world. The extraction of coal is increasing intensively to meet the needs of the ever-increasing population and industries. However, coal mining has resulted in environmental changes, including deforestation, air, water, soil, and landform deterioration. This study investigates the impact of mining on the environment in Ruqigou coalfield by utilising in situ and remote sensing data. Field data collected include temperature, gas compositions, and water samples. Multi-temporal Landsat data of 1991, 2003, and 2019 were used in monitoring the impact of mining on different land covers, especially vegetation. A supervised classification was performed to assess the changes in land cover. In

	order to track the changes in vegetation, normalised difference vegetation index (NDVI) was employed. To study the changes in coal fire areas, thermal anomalies were extracted from the thermal infrared data using a dynamic thresholding technique. The results of in situ analyses show that water quality is unfit for domestic, industrial, and agricultural use. All the gas sampling sites emit noxious gases such as CO_2, CO, NO_2 and degrade the local air quality. The classified maps and vegetation indices show a significant decrease in vegetation. The thermal anomalies show an increase in fire areas over the years. Thus, it could be concluded that the conjunctive use of field-based measurements and remote sensing data can be a powerful tool for gaining a comprehensive understanding of the environmental impacts associated with large-scale mining.
48.	IPCRF: An End-to-End Indian Paper Currency Recognition Framework for Blind and Visually Impaired People M Singh, J Chauhan, MS Kanroo, S Verma, P Goyal - IEEE Access, 2022 **Abstract:** Currency recognition has always been a troublesome task for blind and visually impaired people (BVIP). The problem is more severe in developing countries such as India, where there is still a lack of robust currency recognition systems. BVIP primarily relies on size variations and patterns such as intaglio printings for recognizing the underlying currency denominations. Most of the current Indian legal tenders resemble in size, thus making the identification process more strenuous. Also, the engraved patterns are not as distinctive as BVIP standards, and they fade over time. For an automated paper currency recognition system, issues such as folded or partial views, uneven illumination, and background clutter make it non-trivial and challenging. This paper ventures to present an end-to-end and robust framework for assisting BVIP in recognizing the Indian paper currency denomination. This paper presents a lightweight network, IPCRNet, useful in a resource-constrained environment such as low/medium level smartphones. The proposed network is based on Dense connection, Multi-Dilation, and Depth-wise separable convolution layers. Additionally, we congregated one of the most diversified Indian paper currency image dataset with more than 50,000 images belonging to almost all denominations in circulation. A customized and publically available android application, “Roshni-Currency recognizer”, has also been introduced. The experimental results on multiple datasets demonstrate the superiority of the proposed model. IPCRNet improves the classification accuracy by more than 2% on the proposed dataset compared to the state-of-the-art networks. 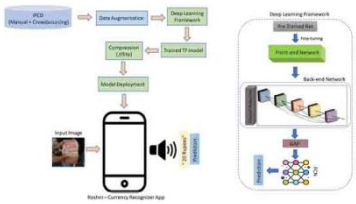
49.	Kerker Condition for Enhancing Emission Rate and Directivity of Single Emitter Coupled to Dielectric Metasurfaces (Advanced Optical Materials 17/2022) M Khokhar, FA Inam, RV Nair - Advanced Optical Materials, 2022 **Abstract:** A quantum metasurface is integrated with a single quantum emitter utilizing Kerker condition to modulate the emission pattern both spectrally and spatially (see article number 2200978 by Megha Khokhar, Faraz A. Inam, and Rajesh V. Nair). A large enhancement of 400

	times in the emission decay rate is achieved at the NV-center zero phonon line wavelength of 640 nm with superior emission directionality. These findings open the door for manipulating single photon emission for applications in quantum photonics, sensing, imaging, and many-body interactions. 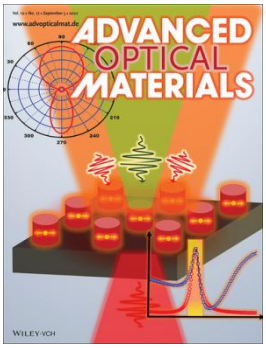
50.	Lattice dynamic stability and electronic structures of ternary hydrides La1−xYxH3 via first-principles cluster expansion P Tsuppayakorn-aek, W Sukmas, P Pluengphon.. R Ahuja - RSC Advances, 2022 **Abstract:** Lanthanum hydride compounds LaH_3 become stabilized by yttrium substitution under the influence of moderate pressure. Novel materials with a wide range of changes in the structural properties as a function of hydrogen are investigated by means of the first-principles cluster expansion technique. Herein, the new compounds $La_{1-x}Y_xH_3$, where $0 \leq x \leq 1$, are determined to adopt tetragonal structures under high-pressure with the compositions $La_{0.8}Y_{0.2}H_3$, $La_{0.75}Y_{0.25}H_3$, and $La_{0.5}Y_{0.5}H_3$. The corresponding thermodynamic and dynamical stabilities of the predicted phases are confirmed by a series of calculations including, for example, phonon dispersion, electronic band structure, and other electronic characteristics. According to the band characteristics, all hydrides except that of $I4_1/amd$ symmetry are semiconductors. The tetragonal $La_{0.5}Y_{0.5}H_3$ phase is found to become semi-metallic, as confirmed by adopting the modified Becke–Johnson exchange potential. The physical origins of the semiconductor properties in these stable hydrides are discussed in detail. Our findings provide a deeper insight into this class of rare-earth ternary hydrides.
51.	Lifetime measurements of states of ^{35}S, ^{36}S, ^{37}S, and ^{38}S using the AGATA γ -ray tracking spectrometer L Grocutt, R Chapman, M Bouhelal.. PP Singh.. - Physical Review C, 2022 **Abstract:** Lifetimes or lifetime limits of a small number of excited states of the sulfur isotopes with mass numbers A=35, 36, 37, and 38 have been measured using the differential recoil-distance method. The isotopes of sulfur were populated in binary grazing reactions initiated by a beam of ^{36}S ions of energy 225 MeV incident on a thin ^{208}Pb target which was mounted in the Cologne plunger apparatus. The combination of the PRISMA magnetic spectrometer and an early implementation of the AGATA γ-ray tracking array was used to detect γ rays in coincidence with projectile-like nuclear species. Lifetime measurements of populated states were measured within the range from about 1 to 100 ps. The number of states for which lifetime measurements or lifetime limits were possible was limited by statistics. For ^{35}S, the lifetime was determined for the first $1/2^+$ state at 1572 keV; the result is compared with a previous published

	lifetime value. The lifetime of the 3^- state of ^{36}S at 4193 keV was determined and compared with earlier measurements. No previous lifetime information exists for the (6^+) state at 6690 keV; a lifetime measurement with large associated error was made in the present work. For ^{37}S, the states for which lifetime limits were established were those at 646 keV with $J\pi=3/2^-$ and at 2776 keV with $J\pi=11/2^-$; there are no previously published lifetime values for excited states of 37S. Finally, a lifetime limit was established for the $J\pi=(6^+)$ state of ^{38}S at 3675 keV; no lifetime information exists for this state in the literature. Measured lifetime values were compared with the results of state-of-the-art shell-model calculations based on the PSDPF, SDPF-U, and FSU effective interactions. In addition, nuclear magnetic-dipole and electric-quadrupole moments, branching ratios, mixing ratios, and electromagnetic transition rates, where available, have been compared with shell-model values. The current work suffers from poor statistics; nevertheless, lifetime values and limits have been possible, allowing a useful discussion of the ability of state-of-the-art shell-model calculations to reproduce the experimental results.
52.	Mapping the landslide susceptibility considering future land-use land-cover scenario A Tyagi, RK Tiwari, N James - Landslides, 2022 **Abstract:** The landslide susceptibility (LS) of any mountainous region is significantly affected by the land-use land-cover (LULC) change. Recently, LULC change effects on landslides have been investigated by many researchers. However, the future prediction of the LS using these LULC changes has not been quantified. The main objective of this study is to predict the future LS map considering the future LULC change scenario for the Tehri region, India. To achieve this objective, we first prepared a geospatial database of past landslide events. These events data were clustered into three major temporal categories, 2005–2010, 2010–2015, and 2015–2020. Second, the artificial neural network (ANN) approach was adopted to prepare LS maps for the years 2010, 2015, and 2020. Then, for the same years, LULC maps were also developed. Third, the future scenario of LULC for the year 2030 was simulated using the ANN-cellular automata model, and the future LULC changes were derived using the change detection technique. Finally, the future LS map for 2030 was projected using derived future LULC changes. The LULC change results reveal that the region is expected to see a significant growth in the built-up area by 34.1%, water body by 6.3%, and agriculture land by 1%. Further, a shrink in dense forest area by 2.4% and sparse forest area by 0.9% is expected in the future. Additionally, the projected LS results reveal a 33% increment in the very high LS zone. This information about the increase in future LS due to rapid urban growth in the mountains can help the various government agencies to scientifically plan the various developmental activities.
53.	Metal-free N-doped carbon catalyst derived from chitosan for aqueous formic acid-mediated selective reductive formylation of quinoline and nitroarenes A Chauhan, A Banerjee, AK Kar, R Srivastava - ChemSusChem, 2022 **Abstract:** A chitosan-derived metal-free N-doped carbon catalyst is synthesized and investigated for selective reductive formylation of quinoline to N-formyl-tetrahydroquinoline and nitroarenes to N-formyl anilides via aqueous HCOOH (FA) mediated catalytic transformation. FA dissociates on the catalyst surface and acts as a hydrogenating and formylating source for selective N-formylation of N-heteroarenes. The carbonized catalyst prepared at 700 °C offered the best activity. A 92% yield of N-formyl-tetrahydroquinoline after 14 h and >99% yield for N-formyl anilide after 12 h at 160 °C were obtained. The excellent catalytic activity is correlated with the type of “N” species and the basicity of the catalyst. Density functional theory (DFT)

	calculations revealed that a water-assisted FA decomposition pathway (deprotonation and dehydroxylation) generates the surface adsorbed -H and -HCOO species, required for the formation of N-formylated products. In addition, the selective formation of N-formyl-tetrahydroquinoline and N-formyl anilides was explained by a comprehensive reaction energetics analysis.
54.	Modeling mRNA translation with ribosome abortions A Jain, AK Gupta - IEEE/ACM Transactions on Computational Biology and Bioinformatics, 2022 **Abstract:** We derive a deterministic mathematical model for the flow of ribosomes along a mRNA called the ribosome flow model with extended objects and abortions (RFMEOA). This model incorporates important cellular features such as every ribosome covers several codons and they may detach from various regions along the track due to more realistic biological situations including phenomena of ribosome-ribosome collisions. We prove that the ribosome density profile along the mRNA in the RFMEOA and in particular, the protein production rate converge to a unique steady-state. Simulations of the RFMEOA demonstrate a surprising result that an increase in the initiation rate may sometimes lead to a decrease in the production rate. We believe that this model could be helpful to provide insight into the effects of premature termination on the protein expression and be useful for understanding and re-engineering the translation process.
55.	Modulation of optical properties of electrochromic device V Agrawal, E Singla, PK Agnihotri - Journal of Materials Science: Materials in Electronics, 2022 **Abstract:** An experimental investigation is carried out to modulate the optical properties of electrochromic devices (ECD) by varying the thickness of electrochromic polymer (ECP) layer. Polyaniline (PANI) is preferred as ECP due to its ability to change colors from light green to green to blue at different voltages. ECDs are fabricated having varying thickness (250–650 nm) of the PANI layer. Topography, morphology, and optical measurements show that the roughness, porosity, and shade of green color depend on the thickness of PANI layer. The effect of ECP layer thickness on the optical performance of ECDs is evaluated through detailed electrochemical, optical, spectroelectrochemical measurements, and spectral colorimetry. ECD shows different shades of green and blue color with higher color contrast for the thicker PANI layer. It is attributed to the roughness and porosity-induced multiple scattering and trapping of incident light in the ECP layer. The reflectance spectra are later used to define the color space for all the ECDs. While the color difference of the ECD fabricated with 250-nm-thick ECP is small, the ECDs prepared using thicker ECP layers show noticeable color difference of greater than 2. Finally, it is shown that varying PANI-based ECP layer thickness is a feasible strategy to modulate the shade of green color in ECDs.
56.	Moments preserving finite volume approximations for the non-linear collisional fragmentation model J Paul, A Das, J Kumar - Applied Mathematics and Computation, 2022 **Abstract:** We present the development of approximate numerical schemes to solve the non-linear fragmentation model. Two numerical weighted finite volume techniques are presented based on the particulate system's mass and number preservation properties. In addition, we have

	extended the results for multi-dimensional formulation. A detailed discussion on mathematical convergence analysis and consistency is exhibited under some regulations on the collision kernels and initial data. It is shown that the developed schemes mathematically possess a second-order convergence rate irrespective of the mesh type. Several numerical examples are presented to validate the proficiency and accuracy of the developed schemes.
57.	Multiobjective Optimization of Chemically Assisted Magnetic Abrasive Finishing (MAF) on Inconel 625 Tubes Using Genetic Algorithm: Modeling and Microstructural Analysis G Singh, H Kumar, HK Kansal.. S Sharma.. - Micromachines (Basel), 2022 **Abstract:** The demand for the surface integrity of complex structures is drastically increasing in the field of aerospace, marine and automotive industry. Therefore, Inconel alloy, due to its superior attributes, has a wide scope for the improvement in surface integrity. To achieve the precise surface finish and enhance the process performance, process optimization is necessary. In current paper, chemically assisted MAF process parameters were optimized using the genetic algorithm (GA) approach during finishing of Inconel 625 tubes. Regression models were developed for improvement in internal surface finish (PIISF), improvement in external surface finish (PIESF), and material removal (MR) using Design expert software. Then, the surface microstructure of Inconel 625 tubes was analyzed using scanning electron microscopy (SEM). ANOVA analysis predicts that processing time and abrasive size have the highest percentage contribution in improving the surface finish and material removal. Multioptimization results suggested to set the level of processing time (A) at 75 min, surface rotational speed (B) at 60 RPM, weight % of abrasives (C) at 30%, chemical concentration (D) at 500 gm/lt and abrasive size (E) at 40 microns to obtain optimal parameters for PIISF, PIESF and MR responses.
58.	Multi-UAV Replacement and Trajectory Design for Coverage Continuity N Gupta, S Agarwal, D Mishra - IEEE International Conference on Communications, 2022 **Abstract:** In this paper, we present a novel framework to maintain coverage continuity in a unmanned aerial vehicle (UAV)-assisted wireless communication system, when a serving UAV runs out of energy. Service continuity is maintained by launching another fully charged UAV to replace the existing serving UAV. This replacement process must ensure maximal coverage to all ground users. Our objective during this replacement process is to maximize the achievable sum rate of all ground users by jointly optimizing the three-dimensional (3D) multi-UAVs trajectory and resource allocation to the users from the individual UAVs. This is carried out in the presence of the UAV's constraints on velocity, collision avoidance, and energy availability while considering a more practical and accurate probabilistic line-of-sight (LoS) channel model. This results in a non-convex optimization problem for which an efficient iterative algorithm based on successive convex approximation and alternating optimization is proposed. Numerical results are provided to obtain insights on the UAV trajectories and the effectiveness of the proposed scheme compared to the existing benchmark schemes is shown.
59.	Neural architecture search for image dehazing M Mandal, YR Meedimale, MSK Reddy, SK Vipparthi - IEEE Transactions on Artificial Intelligence, 2022 **Abstract:** Manual design of deep networks require numerous trials and parameter tuning, resulting in inefficient utilization of time, energy, and resources. In this work, we present a neural architecture search (NAS) algorithm - AutoDehaze, to automatically discover effective

	neural network for single image dehazing. The proposed AutoDehaze algorithm is built on the the gradient based search strategy and hierarchical network-level optimization. We construct a set of search space layouts to reduce memory consumption, avoid the NAS collapse issue, and considerably accelerate the search speed. We propose four search spaces *AutoDehaze*$_{B}$, *AutoDehaze*$_{U1}$, *AutoDehaze*$_{U2}$, and *AutoDehaze*$_{L}$ which are inspired by the boat-shaped, U-shaped, and lateral connection-based designs. To the best of our knowledge, this is a first attempt to present a NAS method for dehazing with a variety of network search strategies. We conduct a comprehensive set of experiments on Reside-Standard (SOTS), Reside-β (SOTS) and Reside- β (HSTS), D-Hazy, and HazeRD datasets. The architectures discovered by the proposed AutoDehaze quantitatively and qualitatively outperform the existing state-of-the-art approaches. The experiments also show that our models have considerably fewer parameters and runs at a faster inference speed in both CPU and GPU devices.
60.	Normal complement problem over a finite field of characteristic 2 H Setia, M Khan - Communications in Algebra, 2022 **Abstract:** –Let *F* be a finite field of characteristic 2. In this article, we have looked into the existence of normal complement of *G* in *V(FG)*, where G is either the alternating group A_4 or the dihedral group D4mD4m of order 4*m*, for an odd integer m≥3. Also, we have explicitly found a normal complement of the symmetric group S_4 in *V(FS4)* over the field *F* containing 2 elements.
61.	Numerical investigation of influence of surface deposition of nanoparticles in tumors during nanofluid injection M Sagar, S Soni, SK Das, H Tyagi - Proceedings of the Thermal and Fluids Engineering Summer Conference, 2022 **Abstract:** In nanoparticle-assisted thermal ablation, the delivery of nanoparticles forms a vital element for attaining optimum temperature elevations in the tumor while sparing surrounding healthy tissue. This paper uses numerical modelling to evaluate the spatiotemporal distributions of nanoparticles inside the tumor region when intra-tumoral/local injection of nanoparticles is considered. The transport of nanoparticles inside the tumor is governed by the advection-diffusion phenomenon combined with porous media theory by considering various flow influencing parameters like injection rate, tumor volume, diffusion rate, nanoparticle size, tissue porosity, and needle diameter. During the injection process, nanoparticles bind on the solid structure of tissue and hence have varying concentration distribution within the tissue. The deposition of nanoparticles is mainly affected by the particle size, local fluid velocity and the structure of the tissue. Obtaining an effective distribution of nanoparticles requires a more detailed understanding of the effect of surface deposition in tissue, and it will be quantified by treating deposition as a concentration dependent reaction. This study evaluates the nanoparticle concentration within the tumor, more specifically, investigates the influence of deposition of particles on the cell surface during infusion of nanoparticles within the tissue. The results indicate that the nanoparticle deposition leads to non-uniform nanoparticles distribution and the nanoparticles concentration decreases on increasing the infusion rate, as the surface deposition of nanoparticles increased by increasing the injection rate.
62.	Numerical Investigation of Photothermal Membrane Distillation D Chamoli, K Garg, SK Das, H Tyagi - Proceedings of the Thermal and Fluids Engineering Summer Conference, 2022

	Abstract: Water is among the most fundamental needs of any society. Studies forecast that by 2030 half of the world's population will be living in areas of high-water stress due to increasing population and water footprint. Desalination can be an alternative to increase the influx of water, and many countries in the Middle East are currently relying on it for their water requirement. The primary desalination techniques are based on phase change of water, due to which they are energy-intensive, which leads to an imbalance of water-energy nexus. Therefore, we need a desalination technique that can run on renewable energy to mitigate the energy footprint. Membrane distillation (MD) is a thermally-driven separation process. It has lots of potentials as it works on lower temperature and pressure range that alternate energy sources can provide. However, the conduction heat loss and temperature polarization in MD make the process less energy efficient. Photothermal membrane distillation (PMD), a process in which the localized heating at the surface of the feed side of the membrane by solar irradiation alone drives the distillation process, can be an effective solution as it eliminates the requirement of input feed heating and lower operating velocity to overcome the problem faced in conventional MD. In this study, the PMD system is modelled mathematical and numerical analysis of the same is carried out for the optimum working performance of the system. Preliminary results indicate that with optimized heat recovery, the performance of the system can be further improved (10%-20%).
63.	Parametric analysis between closed air open water (CAOW) and closed water open air (CWOA) HDH cycles R Beniwal, K Garg, SK Das, H Tyagi - Proceedings of the Thermal and Fluids Engineering Summer Conference, 2022 **Abstract:** Water scarcity affects 88 developing countries where half of the world's population lives. Some of the regions in these countries may require the decentralised supply of freshwater, which may require purification of wastewater, using a low-cost water purification process, driven by waste heat or solar energy, and having less maintenance. Humidification-dehumidification (HDH) desalination has the potential to be the ideal technology for such regions of the world. In this paper, water-heated closed air open water HDH system will be discussed. The performance of this cycle is compared with another configuration of the HDH cycle where water remains in a closed cycle. This paper compares the performance of both these cycles by evaluating gained output ratio (GOR) and distillate production rate (M_d) as a function of the various vital variables related to HDH system. These variables are mass flow rate ratio (m_w/m_a), inlet temperature of saline water, dry bulb and wet bulb temperatures of air, effectiveness of heat and mass exchange devices (humidifier and dehumidifier).
64.	Peptides as diagnostic, therapeutic, and theranostic tools: Progress and future challenges R Thakur, CR Suri, IP Kaur, P Rishi - Critical Reviews™ in Therapeutic Drug Carrier Systems, 2023 **Abstract:** Peptides are emerging as a promising candidate for therapeutic as well as diagnostic applications within the domain of clinical and scientific research. They are recognized for being highly selective, sensitive and efficacious with minimal or no toxicity. Small size, non-immunogenicity, ease of synthesis and huge scope of modification are some of the well-established properties of peptides, which make them an excellent alternative to not only small drug molecules but also to protein-based biopharmaceuticals such as antibodies and enzymes. The attractive pharmacological profile and intrinsic properties of peptides also make them an interesting diagnostic tool for imaging at the molecular and cellular levels. Molecular imaging

	coupled with targeted therapy using peptides as theranostics is a two-edged sword. Besides, traditional peptide formats, multifunctional newer peptide designs with improved pharmacokinetics and targetability are also being explored presently. In this review, we come up with a comprehensive summary of the latest progress on peptides and their potential applications in therapeutics and diagnosis for infectious and non-infectious diseases. The last part of the review discusses suitable carrier systems for the delivery of peptides along with highlighting the future challenges.
65.	Prediction of polyester conductive filter media life on flat and pilot filtration test rigs under flyash aerosol pre-charge S Dutta, A Mukhopadhyay, AK Choudhary, CC Reddy - Journal of Industrial Textiles, 2022 **Abstract:** One of the vital aspects considering the commercial benefit for any gaseous filtration industry is the life cycle of filter material. A filter media providing consistent filtration for a long period of time is desirable for its prolonged life. In view of this; the present study is undertaken for experimental characterization of three different polyester conductive filter materials viz. PTFE coated media, stainless steel fibre blended with PET media, and stainless steel fibre scrim media by predicting their ageing behavior. The materials were investigated on two different laboratory based test rigs viz. flat based and pilot filter unit under two levels of dust densities (50 g/m^3 and 150 g/m^3) using fly ash aerosol. The aerosol was charged through a pre-charger at three levels viz. 4 kV, 8 kV and 12 kV. The outcome revealed an enhanced ageing performance at higher level of aerosol charge in case of both the test rigs for all the materials. However, the relative performance of the flat media test rig has been found to be better under all operating conditions. The ageing behavior of PTFE coated materials has been found to be the best among all the investigated materials in both test rigs due to its better surface characteristics as a result of coating.
66.	Pressure-induced lattice-dynamical stability and superconductivity of ternary pentahydride $MgNiH_5$ P Tsuppayakorn-aek, P Pluengphon, W Sukmas.. R Ahuja.. - International Journal of Energy Research, 2022 **Abstract:** We predict the existence of ternary pentahydride $MgNiH_5$, adopting a hexagonal structure with a space group $P6_3/mmc$, at high pressure. Typically, the clarity of structural-phase stability could be demonstrated by thermodynamical and dynamical stabilities. Herein, we introduce a critical temperature (T_c) superconductivity of the ternary pentahydride, based on the isotropic Éliashberg equation. The T_c is estimated by directly solving the Allen-Dynes equation, with a remarkable value of T_c at 25.6 K. Under the compressing pressure from 100 to 300 GPa, the T_c of $MgNiH_5$ is determined by means of the phonon-mediated superconductivity, arising particularly from a magnitude of partial electron-phonon coupling. Our calculation paves the way for achieving a ratio and a T_c superconductivity in the family of ternary polyhydride.
67.	Pyrophosphate $Na_2CoP_2O_7$ Polymorphs as Efficient Bifunctional Oxygen Electrocatalysts for Zinc–Air Batteries R Gond, S Singh, X Zhao, D Singh, R Ahuja, M Fichtner.. - ACS Applied Materials & Interfaces, 2022 **Abstract:** Developing earth-abundant low-cost bifunctional oxygen electrocatalysts is a key approach to realizing efficient energy storage and conversion. By exploring Co-based sodium

	battery materials, here we have unveiled nanostructured pyrophosphate $Na_2CoP_2O_7$ polymorphs displaying efficient bifunctional electrocatalytic activity. While the orthorhombic polymorph (*o*-NCPy) has superior oxygen evolution reaction (OER) activity, the triclinic polymorph (*t*-NCPy) delivers better oxygen reduction reaction (ORR) activity. Simply by tuning the annealing condition, these pyrophosphate polymorphs can be easily prepared at temperatures as low as 500 °C. The electrocatalytic activity is rooted in the Co redox center with the (100) active surface and stable structural framework as per *ab initio* calculations. It marks the first case of phospho-anionic systems with both polymorphs showing stable bifunctional activity with low combined overpotential (ca. ~0.7 V) comparable to that of reported state-of-the-art catalysts. These nanoscale cobalt pyrophosphates can be implemented in rechargeable zinc–air batteries.
68.	Residual strain engineering in seed layer assisted Kesterite Cu_2ZnSnS_4 absorber layer K Kaur, R Wadhwa, A Ghosh, Nisika, D Kumar, P Kumar, M Kumar - Materials Today Communications, 2022 **Abstract:** Narrow-phase stability of CZTS often leads to the formation of secondary phases and defects that eventually results in disorder in the crystal structure. Moreover, lattice-mismatch and thermal stress at CZTS/Mo interface nourish strained growth, which adversely affects the Cu-Zn ordering in CZTS. Thus far, understanding and evolution of these residual strains and their influence on the optoelectronic properties of CZTS are lacking. Herein, we probed the residual strain along penetration depth and demonstrated a facile approach of tailoring lattice strain in CZTS. High quality CZTS films with seed layer (SL) growth are developed to investigate residual strain distribution using depth-dependent grazing incidence X-ray diffraction (GIXRD) measurements. A graded strain has been identified in SL films than uniformly strained no SL films. Besides improvement in Cu-Zn order, Photoluminescence (PL) signal in SL films was substantially quenched by 55.3%, which is ascribed to the charge transfer as a consequence of graded strain. Graded strain in SL films tends to form multi-homojunction, influencing charge carrier dynamics, resulting in a 36-fold increase in photocurrent and approximately 5 times faster response over No SL CZTS based device. **Graphical Abstract:** 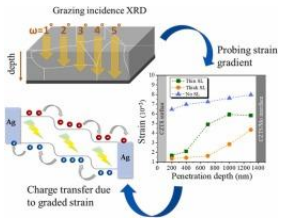
69.	Socio-Demographic Variations in Mode Choice Preferences of Peri-Urban and Urban Areas—A Case Study of Bangalore TM Rahul, A Verma - Proceedings of the Sixth International Conference of Transportation Research Group of India, Conference of Transportation Research Group of India, 2022 **Abstract:** Peri-urban regions are located in the fringes of an existing city and are important in the urban transportation planning process of the city. The present research analyzes the differential impact of socio-demographic factors on the travel behavior of urban and a peri-urban areas. Specifically, the current study, at first, performs a descriptive multivariate mode share

	comparison between motorized two-wheelers and Non-Motorized Transport (NMT). Further, it estimates a mode choice model and a trip distance model to determine the marginal effects of socio-demographic and transportation system characteristics. Interaction terms are introduced in the utility function of the mode choice model using a peri-urban indicator to delineate the differential impact of socio-demographic factors in urban and peri-urban areas. The estimated mode choice model gave a comparatively good fit with the data (47 and 27.5%). The significance of the interaction terms indicated a difference in the influence of travel characteristics between urban and peri-urban areas. Gender has a significant influence on the mode choice with females in both urban and peri-urban region having a positive disposition toward NMT. In both regions, an increase in the travel distance reduced the use of non-motorized modes and increased the use of private vehicles. From a social equity perspective, there was a huge scope for promotion of public transport and non-motorized transport in the peri-urban areas. Further, paratransit could be contemplated as a solution to overcome the poor connectivity in the radial routes of peri-urban areas.
70.	Some remarks on convergence of best proximity points and Semi-cyclic contractions M Gabeleh, G Kosuru - Rendiconti del Circolo Matematico di Palermo Series 2, 2022 **Abstract:** We show that the main conclusions of the recent paper by R. Suparatulatorn et al. [R. Suparatulatorn, W. Cholamjiak and S. Suantai, Existence and convergence theorems for global minimization of best proximity points in Hilbert spaces, Acta Appl. Math., 165, 81-90 (2020)] are not real generalizations but particular cases of convergence of Mann's iteration scheme to a fixed point of a nonexpansive self mapping. As well as the main results of an article by G.K. Jacob et al. [G.K. Jacob, M. Postolache, M. Marudai and V. Raja, Norm convergence iterations for best proximity points of non-self nonexpansive mappings, U.P.B. Sci. Bull., Series A, 79, 49-56 (2017)] which are related to study of convergence of best proximity points for nonexpansive non-self mappings can be concluded, directly, from the convergence results of fixed points for nonexpansive self mappings and so they are not real generalizations. These techniques leads us to introduce a semi-cyclic contractions and therein prove the existence of best proximity points.
71.	Spin and valence variation in cobalt doped barium strontium titanate ceramics A Kaur, D Singh, A Das, Ashokan K, .. R Ahuja - Physical Chemistry Chemical Physics, 2022 **Abstract:** In the present decade, owing to half-metallic ferromagnetism, controlled 3d transition metal-doping based defect engineering in oxide perovskites attracts considerable attention in the pursuit of spintronics. We aim to investigate the electronic structure of Co-doped barium strontium titanate ($Ba_{0.8}Sr_{0.2}Co_xTi_{1-x}O_3$ where x = 0, 0.1, 0.2) solid solution. Structural, vibrational and microscopic properties indicate the cationic substitution of Co at the octahedral Ti position along with a displacive kind of tetragonal-to-cubic phase transformation. X-ray photoelectron spectroscopy evidences the reduction in the valence state from Co^{3+} to Co^{2+} and Ti K edge X-ray absorption spectroscopy endorses the higher lattice symmetry with increasing Co doping. Orbital hybridization triggered electron hopping between O 2p and Co e_g orbitals results in a spin fluctuation from the occupation $t^6_{2g}e^0_g$ for x = 0.1 to the occupation $t^6_{2g}e^1_gL$ for x = 0.20 (L designates a hole in the O 2p shell) aligned state observed from density functional theory calculations. The dominating crystal field energy as compared to intra-atomic exchange (Hund) energy decides the spin-orbital degeneracy for the Co 3d orbital to induce spin fluctuations.

	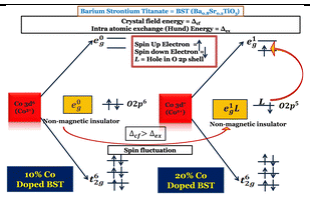
72.	Suitability of turning and grinding steel chips to synthesize metal matrix composite via powder metallurgy route A Singh, A Anand, J Singh, M Singh, K Kumar, P Bhandari, VK Srivastava, A Singh, MK Sinha - Materials Today: Proceedings, 2022 **Abstract:** This research work is inspired by the 3Rs: Reduce; Reuse and Recycle enabling the fabrication of green and clean metal matrix composites. In addition to the environmental benefits, recycling of industrial waste produced by metal machining industry have significant financial advantages. Consequently, the present study aimed to explore suitability of the waste chips produced during turning and grinding operations of mild steel for the fabrication of metal-matrix composite (MMCs) through powder metallurgy (P/M) route have been exhibited. Field emission electron microscopy (FESEM) and Energy-dispersive X-ray spectroscopy (EDS) have been used to evaluate morphology and composition of starting materials Flowability and compressibility of the starting materials have been explored using the Hausner's ratio and Carr's index respectively. The apparent and tapped densities of the mild steel turning chips (MSTCs) 1.88 and 2.17 g/cc. Further in case of steel grinding chips (SGCs) densities were found to be 1.92 and 2.12 g/cc respectively. On the other hand, the on addition of SGCs(0–30 wt%) to the MSTCs the flowability observed to be retarded a bit. Based on the initial investigations it can be concluded that the waste MSTCs and SGC can suitably be processed through P/M to fabricate sustainable MMCs.
73.	Superalkali functionalized two-dimensional haeckelite monolayers: A novel hydrogen storage architecture IJ Jason, Y Pal, Anees P, H Bae.. R Ahuja.. - International Journal of Hydrogen Energy, 2022 **Abstract:** Exploring efficient storage mediums is the key challenge to accomplish a sustainable hydrogen economy. Material-based hydrogen (H_2) storage is safe, economically viable and possesses high gravimetric density. Here, we have designed a novel H_2 storage architecture by decorating graphene-like haeckelite (r57) sheets with the super-alkali (NLi_4) clusters, which bonded strongly with the r57. We have performed van der Waals corrected density functional theory (DFT) calculations to study the structural, electronic, energetic, charge transfer, and H_2 storage properties of one-sided (r57-NLi_4) and two-sided (r57-$2NLi_4$) coverage of r57 sheets. Exceptionally high H_2 storage capacities of 10.74%, and 17.01% have been achieved for r57-NLi_4, and r57-$2NLi_4$ systems, respectively that comfortably surpass the U.S. Department of Energy's (DOE) targets. Under maximum hydrogenation, the average H_2 adsorption energies have been found as −0.32 eV/H_2, which is ideal for reversible H_2 storage applications. We have further studied the effects of mechanical strain to explore the H_2 desorption mechanism. Statistical thermodynamic analysis has been employed to study the H_2 storage mechanism at varied conditions of pressures and temperatures. Our findings validate the potential of r_{57}-$xNLi_4$ as efficient H_2 storage materials.
74.	Two-Dimensional Pentagraphyne as a High-Performance Anode Material for Li/Na-Ion

	Rechargeable Batteries J Deb, R Ahuja, U Sarkar - ACS Applied Nano Materials, 2022 **Abstract:** Recently, we have predicted a two-dimensional (2D) material named pentagraphyne (PG-yne); due to its intriguing properties, it is proposed for a wide range of applications. In this work, we have explored the potentiality of PG-yne as an anode material for Li/Na ion batteries using the density functional theory. Its differential adsorption energy suggests that maximal eight Li/Na ions can be accommodated over the PG-yne surface. We have obtained a high theoretical capacitance of 680 mAh g^{-1} for Li/Na ions adsorbed on PG-yne. The reported theoretical capacitance of PG-yne as an anode material in lithium-ion batteries (LIBs) is moderately higher than that of previously reported 2D anode materials, whereas PG-yne for NIB application has a significantly higher capacitance than that of several previously studied anode materials. Moreover, the low open-circuit voltage along with low diffusion barriers (≤0.50 eV) and much higher electronic conductivity after the adsorption of Li/Na ions again suggest its applicability as an anode material. Further, the molecular transition rate study also confirms the faster diffusivity of Li/Na ions over the PG-yne surface. The high storage capacity and faster diffusion of Li/Na ions adsorbed on PG-yne are mainly due to the lightweight and unique atomic structure of PG-yne. 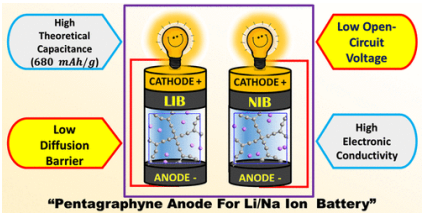
75.	Unraveling the Effect of A-Site Sr-Doping in Double Perovskites $Ca_{2-x}Sr_xScRuO_6$ (x = 0 and 1): Structural Interpretation and Mechanistic Investigations of Trifunctional Electrocatalytic Effects N Kumar, T Rom, M Kumar, TC Nagaiah, E Lee.. - ACS Applied Energy Materials, 2022 **Abstract:** Toward the development of sustainable and clean energy sources for the replacement of fossil fuels, strategies for constructing highly effective and durable trifunctional oxide electrocatalysts with zero emission carbon is a key step for boosting energy technologies through overall water splitting, regenerative fuel cells, and metal–air batteries. Here, two disordered ruthenate double-perovskites Ca_2ScRuO_6 (CSR) and $CaSrScRuO_6$ (CSSR) were synthesized by the conventional high-temperature solid-state reaction method, and their trifunctional electrocatalytic behaviors for the oxygen reduction reaction (ORR) and oxygen and hydrogen evolution reactions (OER/HER) were investigated in alkaline medium (1 M KOH). The orthorhombic (space group *Pbnm*) crystal structures of both CSR and CSSR were refined from the neutron and laboratory X-ray powder diffraction data. The oxidation states of Ru cations in both compounds were shown to be predominantly Ru^{+5}, confirmed by X-ray photoelectron spectroscopy studies. The as-prepared bulk perovskites showed excellent ORR performance with an onset potential of ∼0.89 V for CSR and 0.90 V *vs* reversible hydrogen electrode (RHE) for CSSR, respectively. In addition, both compounds showed significantly low overpotentials toward OER (353 and 323 mV) and HER (313 and 275 mV) at a current density of 10 mA cm^{-2}, demonstrating them to be active trifunctional electrocatalysts. The substitution of an alkaline earth metal at the A-site introduces a synergistic effect of structural distortion and electronic

	properties of Ru^{+5} metal ions responsible for enhanced trifunctional electrocatalytic activities. Such trifunctional catalytic behaviors of CSR and CSSR materials can be further understood by density functional theory (DFT) calculations. The present finding not only provides insight into the catalytic activity of these materials but also presents an example of efficient trifunctional bulk-phase oxide electrocatalysts for practical applications. 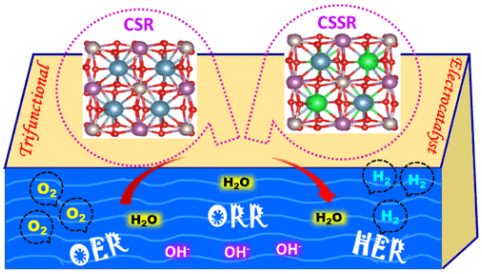
76.	Validity and reliability of polar V800 smart watch to measure cricket-specific movements S Biswas, S Guha, R Bhattacharya - Physical Education Theory and Methodology, 2022 **Abstract:** The study purpose was to assess the reliability and validity of Polar V800 smart watch in measuring various cricket-specific movements. Materials and methods. Only one trained male volunteer was selected to perform all the cricket specific movements to minimize individual error and eliminate between-subject variability. Polar V800 obtained distances were compared with real field markings. Results. Split-half Reliability Statistical method has been used and 'r' score for the measurements taken has been found to be 0.93. 95% confidence intervals also express a good reliability score. The criterion validity method was used to determine the validity of the dataset. The Pearson correlations (r) have been found ranging from 0.86 to 0.99. Predicted best fit line of linear regression has been found as y = 0.9722 X + 0.0046 (where y = observed value, X = real field distance). One way ANOVA followed by Tukey's post hoc test on observed 10m sprint, 20m sprint and run-a-three movements show maximum significant difference with other cricket-specific movements. The mean percentage of bias for all cricket-specific movements has been found to be -2.20 ± 13.17. Conclusions. The study reveals that Polar V800 smart watch has an acceptable accuracy, reliability, and validity for measuring various cricket specific movements with certain limitations.
77.	Vibration attenuation study of curved panel treated with partially constrained composite unaged and aged NBR (Acrylonitrile–Butadiene rubber) elastomers AK Jha, N Kumar, K Suresh - Journal of Vibration Engineering & Technologies, 2022 **Abstract:** Background Reduction in structure vibration by dampers during a defined time has attracted widespread attention in the aerospace and automobile industries. Therefore, the comparative study of curved

panel structure vibration reduction is very important.

Purpose

This paper aims to study the damping effect of a curved panel in the presence of unconstrained and constrained composite NBR elastomeric layers, both unaged and aged (high temperature, low temperature, and QUV).

Methodology

The modal strain energy approach is used to determine placement strategies for elastomeric layer patches. The comparative study shows that the constrained layer damping patches are a more effective way to attenuate vibration for the curved panel when placed at maximum modal strain energy locations. Furthermore, vibration tests of curved panel are conducted by preparing a number of separate samples of unconstrained and constrained composite NBR elastomers patches for each configuration to increase the damping of different modes.

Results and Conclusion

The results show the effectiveness of modal strain energy technique for placement of constrained composite NBR elastomers patches on the curved panel to achieve desired damping characteristics over a broad frequency range. Subsequently, it also demonstrates that, damping of the curved panel is more influenced due to QUV aged elastomeric patches than high and low temperature aged elastomers patches. Moreover, the reduction in damping of the curved panel is more resisted due to the presence of nano carboxylic graphene (CG)/SiO_2 in the aged composite NBR elastomer. The present method elaborates the utility of the technique for placement of constrained elastomeric patches to attenuate structure vibration by modal strain energy and damping reduction resistance against ageing by composite NBR elastomer.

Graphical Abstract:

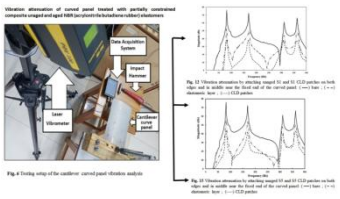

Disclaimer: This publication digest may not contain all the papers published. Library has compiled the publication data as per the alerts received from Scopus and Google Scholar for the affiliation "Indian Institute of Technology Ropar" for the month of September 2022. The author(s) are requested to share their missing paper(s) details if any, for the inclusion in the next publication digest.